

SUPPLEMENTARY INFORMATION

Rapid Translocation of Nanoparticles from the Lung Airspaces to the Body

Hak Soo Choi¹, Yoshitomo Ashitate¹, Jeong Heon Lee¹, Soon Hee Kim¹, Aya Matsui¹, Numpon Insin²,
Moungi G. Bawendi², Manuela Semmler-Behnke³, John V. Frangioni^{1,4,*}, and Akira Tsuda^{5,*}

¹ Division of Hematology/Oncology, Department of Medicine and ⁴ Department of Radiology,
Beth Israel Deaconess Medical Center, Boston, MA 02215

² Department of Chemistry, Massachusetts Institute of Technology, Cambridge, MA 02139

³Institute of Lung Biology and Disease, Helmholtz Center München - German Research Center for
Environmental Health, Neuherberg/Munich 85764, Germany

⁵ Molecular and Integrative Physiological Sciences, Harvard School of Public Health,
Boston, MA 02115

The Supplementary Information includes:

Supplementary Figure 1. TEM Images of the Core of Different Sized INPs

Supplementary Figure 2. Physical and Optical Properties of NPs in PBS and 100% Serum

Supplementary Figure 3. Experimental Setup and Operation of the Double-lumen Balloon Catheter

Supplementary Figure 4. Biodistribution of INP1 (5 nm HD; 800 nm; NIR Channel #2) and ONP6 (120 nm HD; 700 nm; NIR Channel #1) in a SD Rat

Supplementary Figure 5. Biodistribution of ^{99m}Tc-conjugated INP1 (a) and ONP1 (b) into SD Rats

Supplementary Figure 6. Lung Instillation of 10 pmol/g of ONP1 in a SD Rat

Supplementary Video 1. Real-Time Translocation of NPs from the Lung to a Mediastinal Lymph Node

Supplementary Video 2. Real-Time Clearance of NPs from Kidneys to Bladder

Synthesis of INP1 – INP4: All chemicals and solvents were of American Chemical Society or HPLC purity and were purchased from Sigma-Aldrich (Saint Louis, MO, USA) unless otherwise specified. CdSe(ZnCdS) core(shell) quantum dots (QDs) with emission wavelength of 545 nm were synthesized as previously described.¹⁻⁵ Briefly, the core stock solution was centrifuged and re-dispersed in hexane, filtered through a 0.2 μm filter, and injected into a degassed solution of 99% trioctylphosphine oxide (10 g) and n-hexylphosphonic acid (0.4 g). Precursor solutions of ZnEt_2 and $(\text{TMS})_2\text{S}$ were prepared by dissolving the appropriate amounts of each in 4 mL of trioctylphosphine and loading them into two separate syringes under an inert atmosphere. The precursor solutions were injected simultaneously into a 130°C bath at a rate of 4 mL/h and annealed overnight at 80°C.

Ligand exchange with cysteine was carried out using a biphasic exchange method, in which the QDs were size-selectively precipitated twice using acetone and were then re-dispersed in CHCl_3 . Next a solution of cysteine (40 mg/mL) in phosphate-buffered saline (PBS), pH 7.4 was added. This biphasic mixture was stirred vigorously for 2–6 h until the organic layer became colorless. After removing the organic solvent, the QDs were precipitated twice with the addition of ethanol and re-dispersed in PBS, pH 7.4. The cysteine-coated QDs were stabilized by adding dithiothreitol (DTT, 1 mM). They remained stable for more than one month and exhibited high quantum yields (QY) of $\approx 28\%$. INP1 was synthesized via NHS ester chemistry with CW800 (LI-COR, Lincoln, NE) in PBS, pH 7.8 (labeling ratio ≈ 1.4).

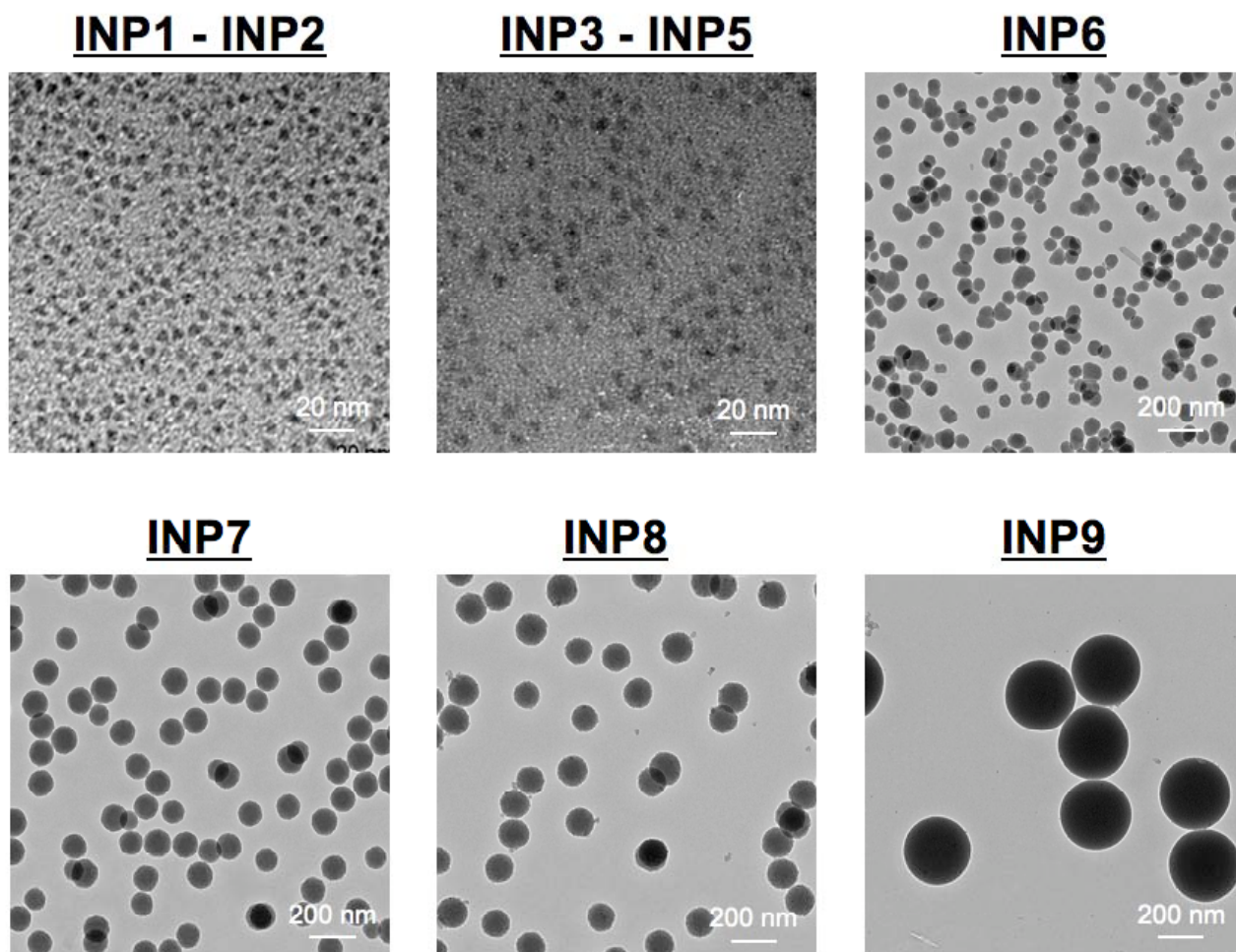
Ligand exchange with a dihydrolipoic acid (DHLA)-conjugated polyethylene glycol spacer (DHLA-PEG, MW 1 kDa) was performed according to reported procedures.^{6,7} Briefly, an aliquot of QD growth solution (0.2 mL) was precipitated with the addition of acetone followed by centrifugation, the supernatant was discarded, and 50 μL of DHLA-PEG along with 50 μL of MeOH was added to the pellet. The mixture was stirred at 60°C for 2 h and precipitated with the addition of ethanol, chloroform, and hexane followed by centrifugation. The supernatant was discarded and the QD sample was re-dispersed in PBS, pH 7.4 for analysis. For engineering INP2, 1 mM DHLA was added for conjugating CW800 in PBS, pH 7.8, resulting in a labeling ratio of 1.8. The labeling ratio was calculated using the extinction coefficients of QD ($\epsilon_{530\text{nm}} = 56,800 \text{ M}^{-1} \text{ cm}^{-1}$) and CW800 ($\epsilon_{785\text{nm}} = 240,000 \text{ M}^{-1} \text{ cm}^{-1}$).

CdTe(ZnS) QDs with carboxylated PEG (INP3) and amino PEG coatings (INP4), supplied at 8 μM in borate buffer (50 mM borate, pH 8.3), were purchased from Invitrogen Corporation (QDot 800 ITK, Carlsbad, CA). The original HD was found to be 16 nm in PBS, pH 7.4, while a 10 to 15 nm increase in HD was observed after 1 h serum incubation at 37°C. INP5 was prepared by conjugating 3.4 kDa of α -amino- ω -carboxylic acid PEG (NH_2 -PEG-COOH, Nektar, San Carlos, CA) on the carboxyl surface of INP3 via conventional EDC chemistry. Briefly, carboxylated QDs (8 μM) were resuspended

in 0.1 M 2-(N-morpholino)ethanesulfonic acid (MES) at pH 6, and treated with carbodiimide 1-ethyl-3-(3-dimethylaminopropyl) carbodiimide (EDC; Pierce) and sulfo-NHS (Pierce). The suspension was incubated for 15 min and excess reagents removed by ultrafiltration. 100 μ M of NH₂-PEG-COOH was dissolved in PBS, pH 8.0 and mixed with the MES solution. After a 3 h reaction, the mixtures were subjected to ultrafiltration with Tris (pH 8.0) to quench unreacted NHS ester.

Synthesis of INP6 – INP9: A size series of silica nanospheres of 50-300 nm in diameter were purchased from Polyscience, Inc (Warrington, PA). CdSe(ZnS) core(shell) QDs incorporated silica NPs (INP6 - INP9) were prepared using the method previously described.⁸ CW800 NIR fluorophores were conjugated to these silica nanospheres in two steps: 1) amine functionalization of the silica surface followed by 2) coupling with NHS ester dyes. In a typical procedure for amine functionalization, 10 to 30 mg silica nanospheres were dispersed into 10 mL of ethanol by sonication. 500 μ L of (3-aminopropyl)trimethoxysilane were added into the reaction mixture, followed by adding 50 μ L of H₂O and 50 μ L of NH₄OH. The mixture was stirred at room temperature for 1 h, centrifuged, the supernatant discarded, and the nanospheres re-dispersed in ethanol. In order to couple the NIR dye, amine-functionalized nanospheres were sonicated in PBS (pH 7.8) for 15 min, and 200 equiv of CW800 NHS ester were added into the mixture. The reaction mixture was stirred at room temperature for 2 h. The final NIR-emitting nanospheres were purified by centrifugation. The surfaces of these nanospheres were mostly covered with native, un-reacted silanol groups and the coupled NIR dye molecules.

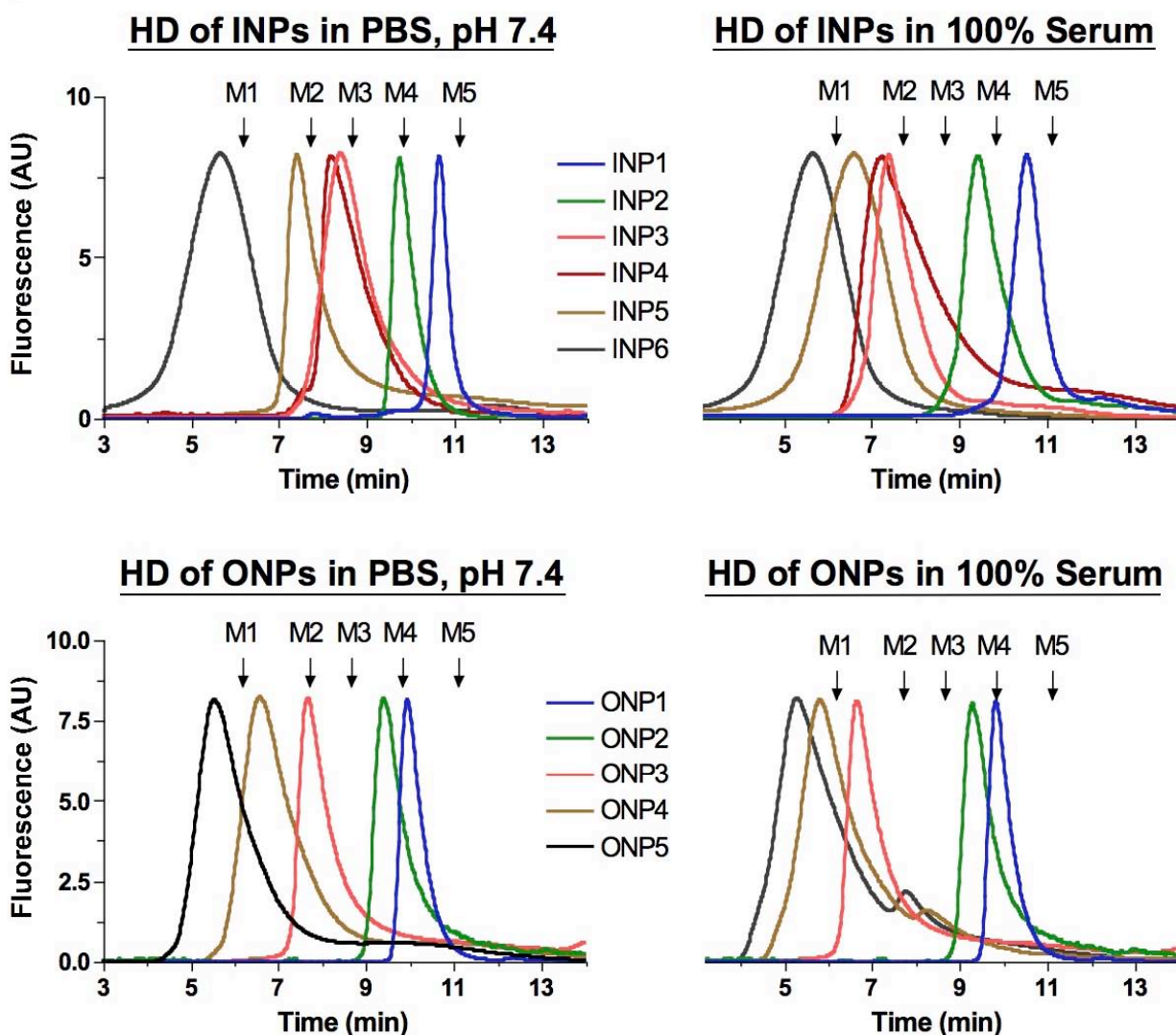
Transmission Electron Microscope (TEM): The size of the INP core(shell) structures was determined using a JEOL 200CX TEM operating at 200 kV. One drop of a dilute sample of INPs in hexane, prepared after one precipitation, was placed onto a Formvar-coated copper grid, allowed to settle for 20 seconds, and wicked away using an absorbent tissue. Size analysis was performed on captured digital images using ImageJ.



Supplementary Figure 1 - TEM Images of the Core of Different Sized INPs: INP1 and INP2 ($3.2 \text{ nm} \pm 1.1 \text{ nm}$), INP3 - INP5 ($8.4 \pm 1.9 \text{ nm}$), INP6 ($52 \text{ nm} \pm 6 \text{ nm}$), INP7 ($114 \pm 9 \text{ nm}$), INP8 ($133 \pm 6 \text{ nm}$), and INP9 ($323 \pm 11 \text{ nm}$).

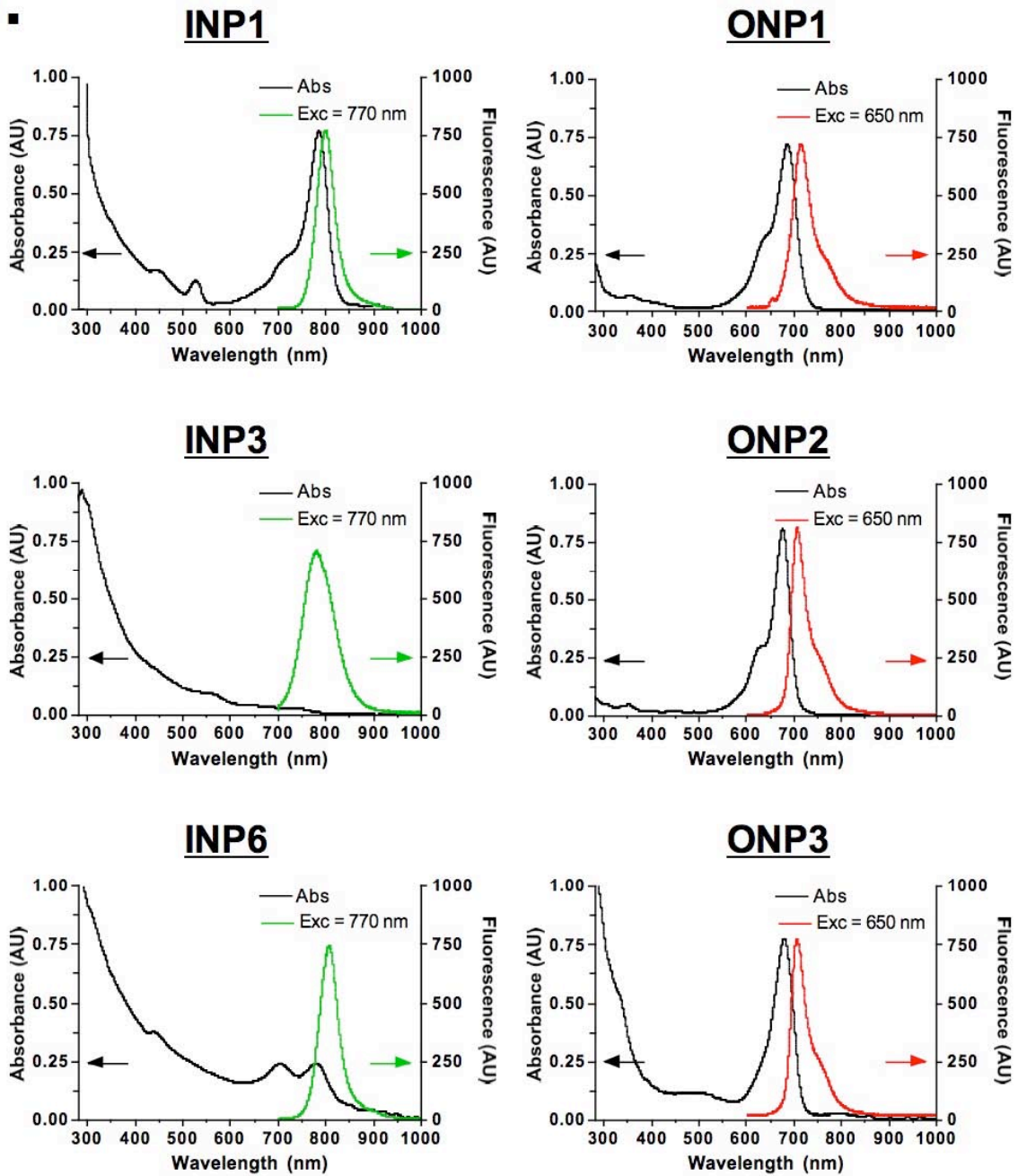
Synthesis of Organic Nanoparticles (ONPs): ONP1 was prepared by a reaction of Cy5.5-NHS (Amersham Biosciences) with human serum albumin (HSA; American Red Cross, Washington, DC), followed by purification by gel filtration chromatography (GFC) using Econo-Pac P6 cartridges (Bio-Rad, Hercules, CA) with a flow rate of 1 mL/min (mobile phase = PBS, pH 7.4). The labeling ratio was 2.6, which was estimated using the extinction coefficients of HSA ($\epsilon_{280\text{nm}} = 32,900 \text{ M}^{-1}\text{cm}^{-1}$) and Cy5.5 ($\epsilon_{675\text{nm}} = 19,000 \text{ M}^{-1}\text{cm}^{-1}$). ONP2 was synthesized by simply mixing two equiv of Cy5.5-NHS with amino mPEG 20 kDa (Nektar) in PBS at pH 7.8, followed by GFC purification using P6 cartridges (labeling ratio = 1). A size series of nanospheres of polystyrene and polyacrylate block copolymers were purchased from Phosphorex, Inc. (Fall River, MA) and modified to emit 700 nm NIR fluorescence by conjugating Cy5.5 with 5 to 10 labeling ratio (ONP3 - ONP7).

a.



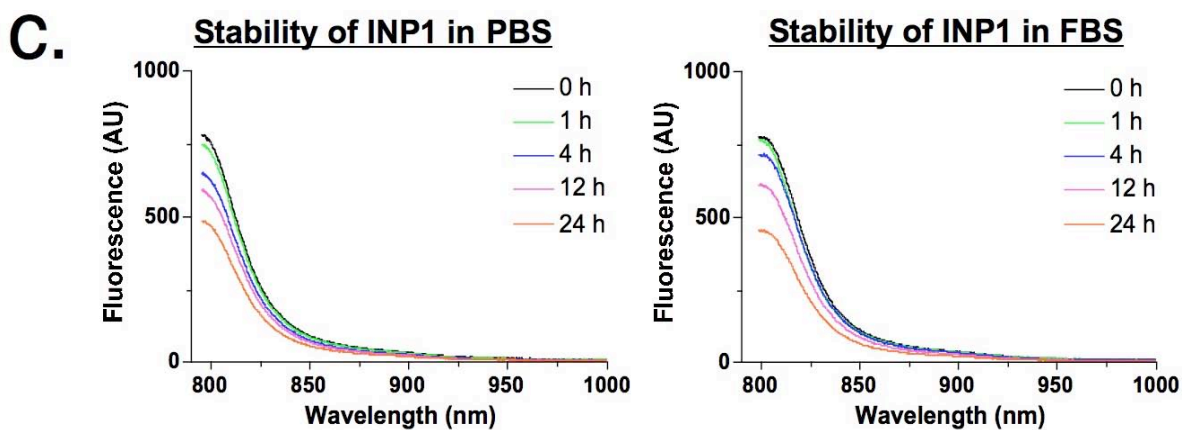
Supplementary Figure 2a – Physical and Optical Properties of NPs in PBS and 100% Serum: HD of INPs and ONPs by GFC in PBS (pH 7.4) and 100% serum. Fluorescence at the peak emission wavelength is shown for each tracer. Molecular weight markers M1 (blue dextran; 2 MDa, 43.4 nm HD), M2 (thyroglobulin; 669 kDa, 18.8 nm HD), M3 (γ -globulin; 158 kDa, 11.1 nm HD), M4 (ovalbumin; 44 kDa, 6.1 nm HD), and M5 (myoglobin; 17 kDa, 3.8 nm HD) are shown by arrows.

b.



Supplementary Figure 2b – Physical and Optical Properties of NPs in PBS and 100% Serum:

Absorption and emission fluorescence spectra of INPs (excitation = 770 nm) and ONPs (excitation = 650 nm) in 100% serum.



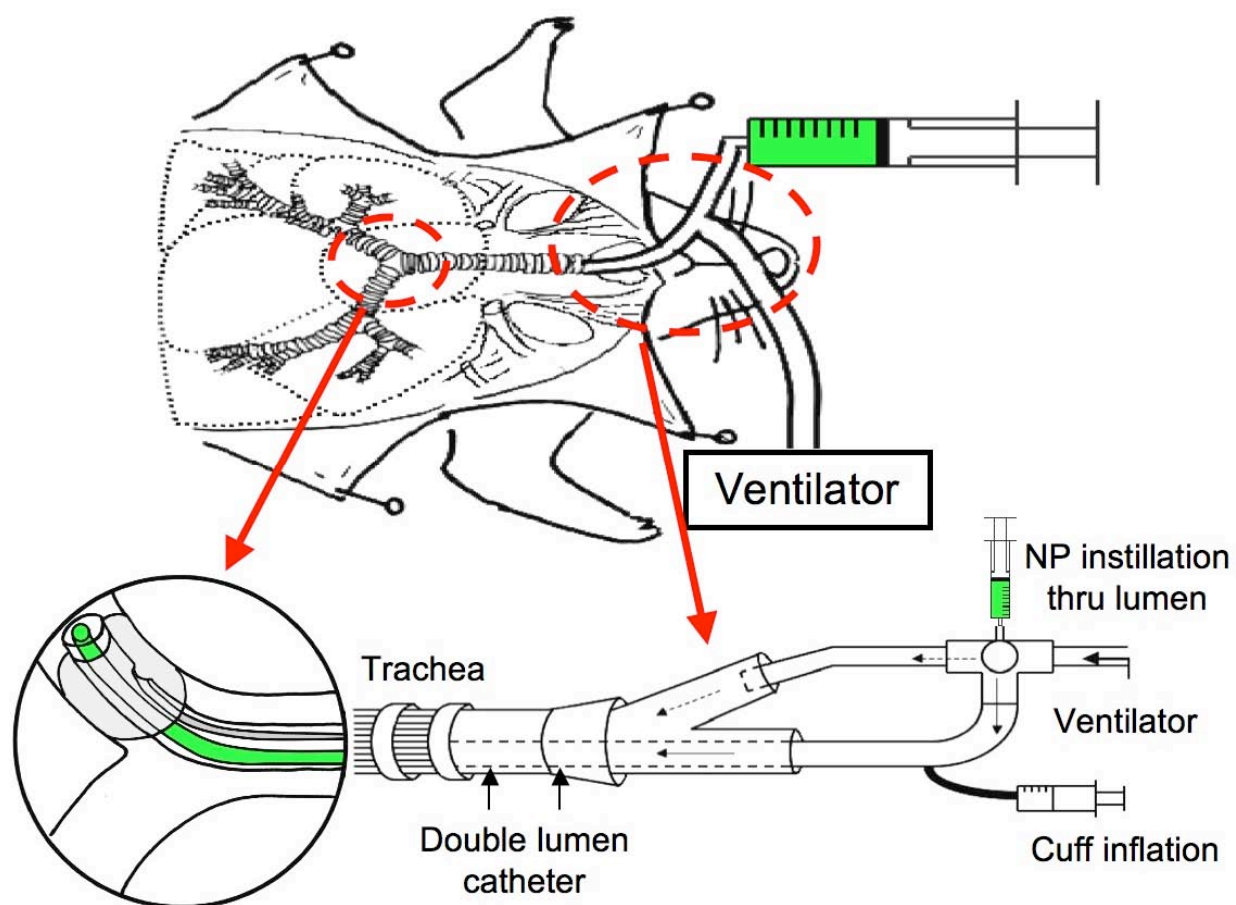
Stability	0 h	1 h	4 h	12 h	24 h
INP1 in PBS (%)	100.00	95.18	82.86	75.40	62.59
INP1 in FBS (%)	100.00	95.22	91.68	77.18	58.82

Supplementary Figure 2c – Physical and Optical Properties of NPs in PBS and 100% Serum: Optical stability of INP1 in PBS and 100% fetal bovine serum (FBS) over 24 hr at 37 °C.

Gel-Filtration Chromatography (GFC): Gel-filtration analysis with on-line full spectrum (300 - 1000 nm) absorbance and fluorescence spectrometry was performed as described in detail previously.¹ For measurement of the effect of serum protein adsorption, 1 μ M NPs were incubated in PBS and 100% rat serum for 1 h at 37°C prior to loading 100 μ L on an 8 \times 300 mm, 200 Å Diol size-exclusion column (SEC, YMC, Japan). For the mobile phase, PBS, pH 7.4 was used with a flow rate of 0.8 mL/min. Calibration of HD was performed by injecting 100 μ L of protein standards containing blue dextran (M1, 2 MDa, 43.4 nm HD), thyroglobulin (M2, 669 kDa, 18.8 nm HD), γ -globulin (M3, 158 kDa, 11.9 nm HD), ovalbumin (M4, 44 kDa, 6.13 nm HD), and myoglobin (M5, 17 kDa, 3.83 nm HD). All HD measurements were performed three times in independent experiments.

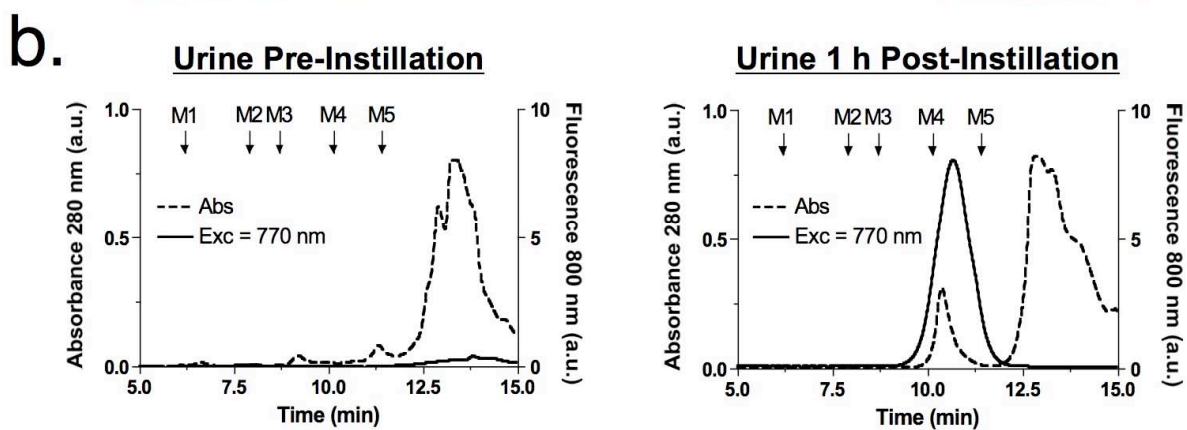
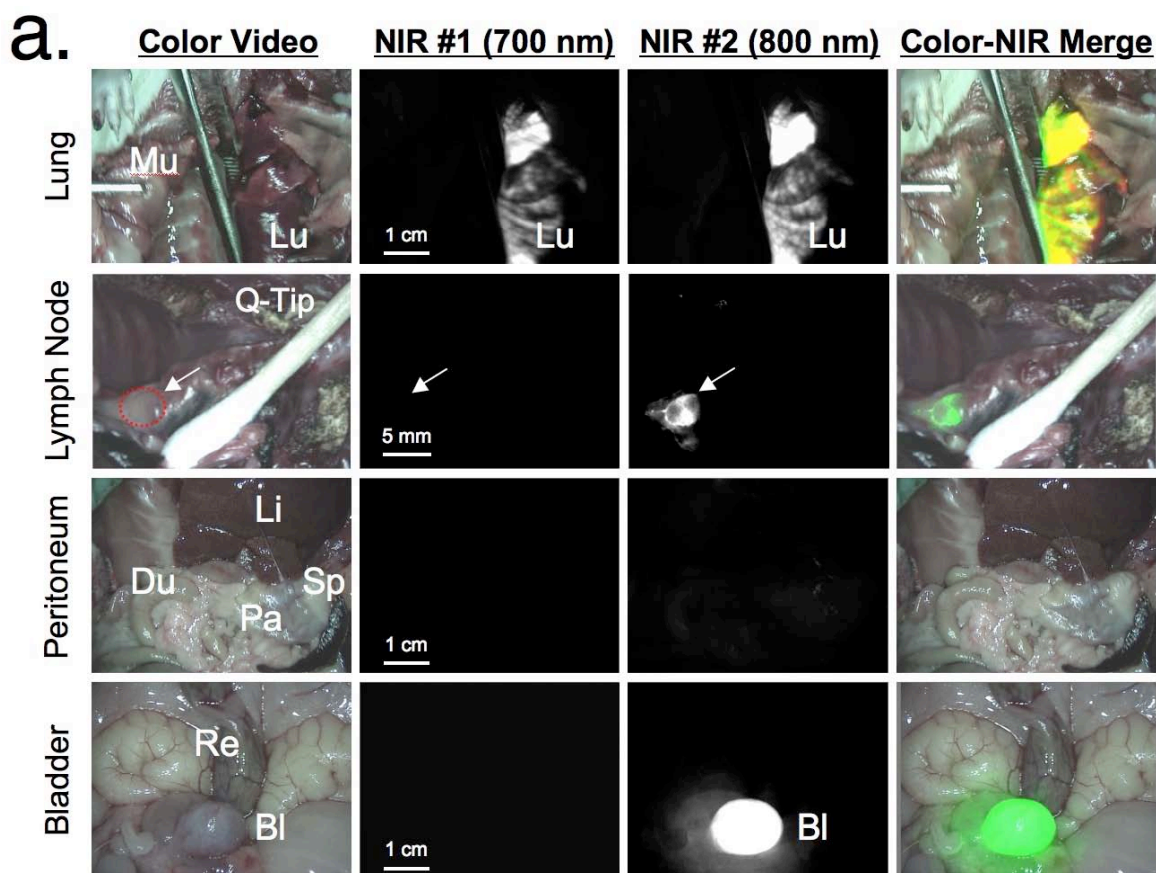
Real-Time Intraoperative Fluorescence Imaging System: Details for the FLARE™ (Fluorescence-Assisted Resection and Exploration) imaging system are as follows. For fluorescence excitation, twenty four custom 1” 670 nm LED modules fitted with 667 ± 11 nm excitation filters and twenty nine 760 nm 1” LED modules fitted with 760 ± 20 nm excitation filters were constructed as described in detail previously.^{9,10} White light was provided by eight 1” LED modules fitted with 650 nm shortpass filters. In order to observe the movement of NPs over time, mediastinal LNs were carefully exposed without disturbing blood flow and lymphatics. A series of NP mixtures (800 nm NIR INPs and 700 nm NIR ONPs; minimized volume: 50 - 100 μ L) was instilled into the right lung of a Sprague-Dawley (SD) male rat using a specially designed double-lumen balloon catheter. A thru lumen was used for administration

of NPs and for ventilation of the right lung. An inflated balloon was used to block mucociliary clearance backflow of administered NPs back to the trachea, because backflow would induce high background signals interfering with clear imaging of the mediastinal LNs. Both lungs were ventilated for one hour (**Supplementary Fig. 3**).



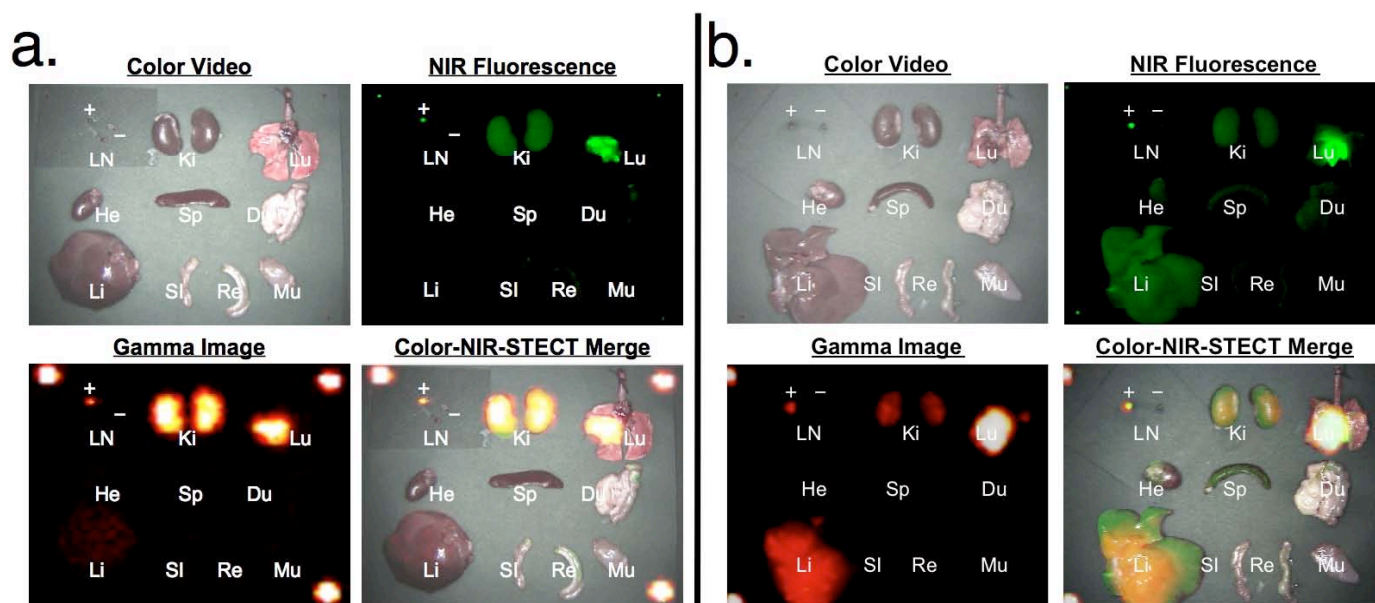
Supplementary Figure 3 – Experimental Setup and Operation of the Double-lumen Balloon Catheter: Gray indicates the balloon used to block mucociliary flow back into the trachea while the animal is being ventilated through the thru lumen. Green indicates the NP solution.

As shown in **Supplementary Figure 4**, a significant portion of the ultra small NPs (800 nm emitting INP1, 5 nm HD) were found in the LNs and bladder 1 h post-instillation, suggesting that INP1 passed through the kidneys and accumulated in urine, while no translocation from lungs neither to LNs or to the bladder was observed with larger NPs (700 nm emitting ONP6, 97 nm HD). In addition, there were almost no accumulation of INP1 (nor ONP6) in the liver, spleen, and intestine because of the zwitterionic surface coating of the ultra small INP1.¹



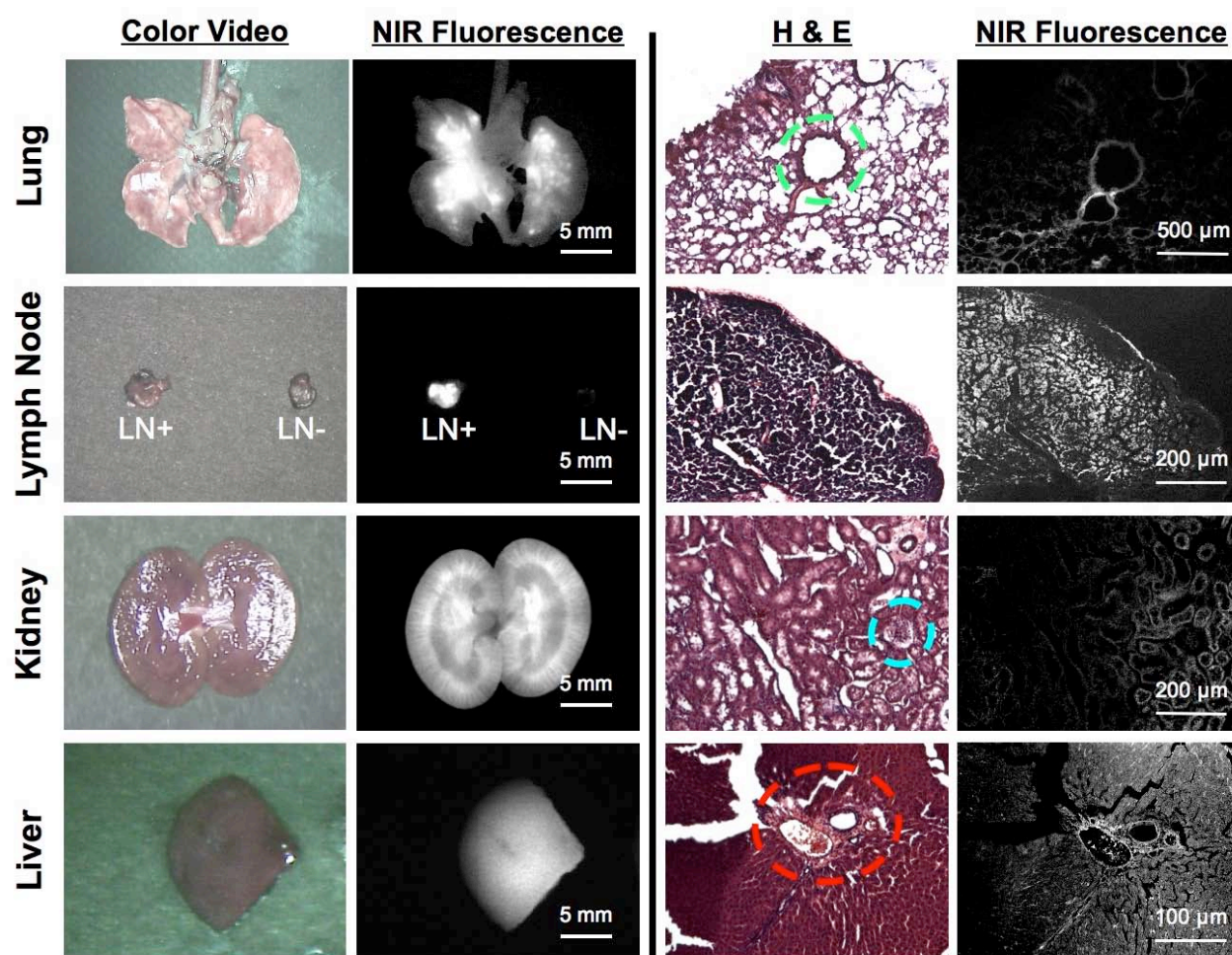
Supplementary Figure 4 – Biodistribution of INP1 (5 nm HD; 800 nm; NIR Channel #2) and ONP6 (120 nm HD; 700 nm; NIR Channel #1) in a SD Rat: (a) 10 pmol/g of each NPs were administered intratracheally. Shown are color video, NIR channel #1 (red pseudo-color), NIR channel #2 (lime green pseudo-color), and a pseudo-colored merge of the three taken 1 h post-instillation. Abbreviations used are Bl: bladder; Du: duodenum; Li: liver; Lu: lung; LN: lymph node; Mu: muscle; Pa: pancreas; Sp: spleen; and Re: rectum. Arrows and red dotted circle indicate LN. $\lambda_{Exc} = 667 \pm 11$ nm and $\lambda_{Em} = 700 \pm 17.5$ nm for NIR #1. $\lambda_{Exc} = 760 \pm 20$ nm and $\lambda_{Em} = 795$ nm longpass for NIR #2. (b) Urine collected pre- and post-administration of INP1, and analyzed by GFC. Tracings include absorbance at 280 nm (dotted curve) and fluorescence at 800 nm (solid curve, $\lambda_{Exc} = 770$ nm). Molecular weight markers M1 (blue dextran; 43.4 nm HD), M2 (thyroglobulin; 18.8 nm HD), M3 (γ -globulin; 11.1 nm HD), M4 (ovalbumin; 6.1 nm HD), and M5 (myoglobin; 3.8 nm HD) are shown by arrows.

^{99m}Tc-Labeling of INPs and Radioscintigraphic Imaging: ^{99m}Tc-conjugated INPs were prepared using high-specific-activity *N*-hydroxysuccinimide (NHS) ester of ^{99m}Tc-MAS₃ (MAS₃ is *S*-acetylmercaptoacetyltriserine) as described previously.^{1,4,5} Briefly, 80 μL of ^{99m}Tc-MAS₃-NHS (2 mCi) in DMSO was added to 1 mL of INP1 or INP4 solution (9 μM) in PBS, pH 7.8. For ^{99m}Tc-INP3 conjugation, 1 mM cysteine was supplemented into INP3 solution before adding ^{99m}Tc-MAS₃ solution. After stirring for 1 h, the radiolabeled conjugates were purified by washing five times in Vivaspin concentrators (MWCO 5,000) with pH 7.4 PBS and analyzed by RP-HPLC on a 8 x 300 mm, 200 Å Diol (YMC, Kyoto, Japan) size-exclusion column using PBS, pH 7.4 as mobile phase. Samples were administered into lungs through a custom-built catheter as described in the manuscript. Because of the small volume in which the dose was administered, the volume of dead space inherent to the catheter, and the inability to flush the dead space since it would introduce excess fluid into the lungs, 24.1 ± 7.4 % of the dose applied to the catheter's Luer-lock was retained in the catheter. The activity remaining in the catheter was measured for each experiment and the net injected dose used for all calculations was the dose applied to the Luer-lock of the catheter minus the retained dose in catheter's dead space.



Supplementary Figure 5 – Biodistribution of ^{99m}Tc-Conjugated INP1 (a) and ONP1 (b) into SD Rats: Shown are the color video (top left), NIR fluorescence (top right), gamma camera images (bottom left), and merged image of the three (bottom right) of resected organs at 1 h post-instillation. Abbreviations used are: LN+, posterior mediastinal LN; LN-, negative para-aortic LN; Ki, kidneys; Lu, lungs; He, heart; Sp, spleen; Du, duodenum; Li, liver; SI, small intestine; Re, rectum; and Mu, muscle.

Histological Analysis of Tissues: In case of INP1 (Fig. 2b), the most intense signals in the lung were found around the bronchioles and alveoli, which means the majority of NPs administered into the bronchus remained on the surface of bronchioles and alveoli, and then entered the interstitium. In the LNs, strong fluorescence was measured through the entire tissue. Interestingly, INP1 was detected only in the kidneys and not in the liver because of its small HD and zwitterionic surface characteristics.¹ Additionally, we prepared histological samples of ONP1 as shown in **Supplementary Figure 6**. In contrast to INP1, strong signal was detected in the liver, specifically in the portal area (red dotted circle) including portal vein, hepatic artery, and bile duct. This suggests that ONP1 was being excreted through the hepatobiliary clearance route at 1 h post-administration.



Supplementary Figure 6 – Lung Instillation of 10 pmol/g of ONP1 in a SD Rat: Frozen sections were obtained from resected organs at 1 h post-administration. Abbreviations used are: LN+, posterior mediastinal LN; and LN-, negative para-aortic LN. Also shown are representative histological images from the same organ/tissue obtained during histological analysis of frozen sections (right two panels). Green dotted circle = bronchiole; blue dotted circle = glomerular basement membrane; red dotted circle = portal area (portal vein, hepatic artery, and bile duct). All NIR fluorescence images ($\lambda_{Exc} = 667 \pm 11$ nm and $\lambda_{Em} = 700 \pm 17.5$ nm) have identical exposure times and normalizations.

REFERENCES

1. Choi, H.S. et al. Renal clearance of quantum dots. *Nat Biotechnol* **25**, 1165-1170 (2007).
2. Liu, W. et al. Compact cysteine-coated CdSe(ZnCdS) quantum dots for in vivo applications. *J Am Chem Soc* **129**, 14530-14531 (2007).
3. Dabbousi, B.O. et al. (CdSe)ZnS core-shell quantum dots: synthesis and characterization of a size series of highly luminescent nanocrystallites. *J Phys Chem B* **101**, 9463-9475 (1997).
4. Choi, H.S. et al. Tissue- and organ-selective biodistribution of NIR fluorescent quantum dots. *Nano Lett* **9**, 2354-2359 (2009).
5. Choi, H.S. et al. Design considerations for tumour-targeted nanoparticles. *Nat Nanotechnol* **5**, 42-47 (2010).
6. Uyeda, H.T., Medintz, I.L., Jaiswal, J.K., Simon, S.M. & Mattoussi, H. Synthesis of compact multidentate ligands to prepare stable hydrophilic quantum dot fluorophores. *J Am Chem Soc* **127**, 3870-3878 (2005).
7. Mattoussi, H. et al. Self-assembly of CdSe-ZnS quantum dot bioconjugates using an engineered recombinant protein. *J Am Chem Soc* **122**, 12142-12150 (2000).
8. Insin, N. et al. Incorporation of iron oxide nanoparticles and quantum dots into silica microspheres. *ACS Nano* **2**, 197-202 (2008).
9. Troyan, S.L. et al. The FLARE™ intraoperative near-infrared fluorescence imaging system: a first-in-human clinical trial in breast cancer sentinel lymph node mapping. *Ann Surg Oncol* **16**, 2943-2952 (2009).
10. Gioux, S. et al. High-power, computer-controlled, light-emitting diode-based light sources for fluorescence imaging and image-guided surgery. *Mol Imaging* **8**, 156-165 (2009).

SUPPLEMENTARY VIDEOS

Supplementary Video 1 Real-time translocation of NPs from the lung to a mediastinal lymph node. 10 pmol/g of INP1 (left bottom, pseudo-colored in lime green in Color-NIR Merge) and ONP6 (right top, pseudo-colored in red in Color-NIR Merge) were administered intratracheally into a 500 g SD rat. Shown are color video (left top), NIR channel #1 (right top), NIR channel #2 (left bottom), and a pseudo-colored merge of the three (right bottom) taken over 30 min. Abbreviations used are: He, heart; Lu, lung; and Mu, muscle. Arrows and red circle indicate lymph node. $\lambda_{\text{Exc}} = 667 \pm 11$ nm and $\lambda_{\text{Em}} = 700 \pm 17.5$ nm for NIR channel #1. $\lambda_{\text{Exc}} = 760 \pm 20$ nm and $\lambda_{\text{Em}} = 795$ nm longpass for NIR channel #2.

Supplementary Video 2 Real-time clearance of NPs from kidneys to bladder. 10 pmol/g of INP1 (left bottom, pseudo-colored in lime green in Color-NIR Merge) and ONP6 (right top, pseudo-colored in red in Color-NIR Merge) were administered intratracheally into a 500 g SD rat. Shown are color video (left top), NIR #1 (right top), NIR channel #2 (left bottom), and a pseudo-colored merge of the three (right bottom) taken at 1 h post-administration. Abbreviations used are: Bl, bladder; Ki, kidney; Re, rectum; and Sp; spleen. Arrows indicates left ureter. $\lambda_{\text{Exc}} = 667 \pm 11$ nm and $\lambda_{\text{Em}} = 700 \pm 17.5$ nm for NIR channel #1. $\lambda_{\text{Exc}} = 760 \pm 20$ nm and $\lambda_{\text{Em}} = 795$ nm longpass for NIR channel #2.